Catalysis Letters (2023) 153:3569–3580
https://doi.org/10.1007/s10562-023-04273-7

Graphene Encapsulated Low-Load Nitrogen-Doped Bimetallic Magnetic Pd/Fe@N/C Catalyst for the Reductive Amination of Nitroarene Under Mild Conditions

Shanshan Lin[1,3] · Jianguo Liu[2] · Longlong Ma[2]

Received: 11 November 2022 / Accepted: 2 January 2023 / Published online: 20 January 2023

Abstract

Aniline is a group of important platform molecules that has been widely used in the synthesis of other high-value chemicals and pharmaceutical products. How to produce high-value anilines as the high-value chemical intermediates more efficiently and environmentally has always been a research topic in the industry. Catalytic hydrogenation is an environmentally friendly method for preparing halogenated anilines. Traditional noble metal catalysts face the problems of cost and noble metals residue. To improve the purity of the product as well as the activity and recyclability of the catalyst, we prepared a Pd/Fe magnetic bimetallic catalyst supported on N-doped carbon materials to reduce nitrobenzene to aniline under mild conditions. The catalyst has a low Pd loading of 2.35%. And the prepared bimetallic Pd/Fe@N/C catalyst showed excellent catalytic reactivity with the nitrobenzene conversion rate of 99%, and the aniline selectivity of 99% under mild reaction conditions of 0.8 MPa H_2 and 40 °C. A variety of halogenated and aliphatic nitro compounds were well tolerated and had been transformed to the corresponding target amine products with excellent selectivity. In addition, the novel N-doped graphene-encapsulated bimetallic magnetic Pd/Fe@N/C catalyst not only had magnetic physical properties, which was easy to separate, recover, and used for the recycling of the catalyst without metal leaching but also catalyzed highly selective reductive amination of aromatics was a green, economical and environmentally friendly reaction with the only by-product of H_2O.

Graphical Abstract

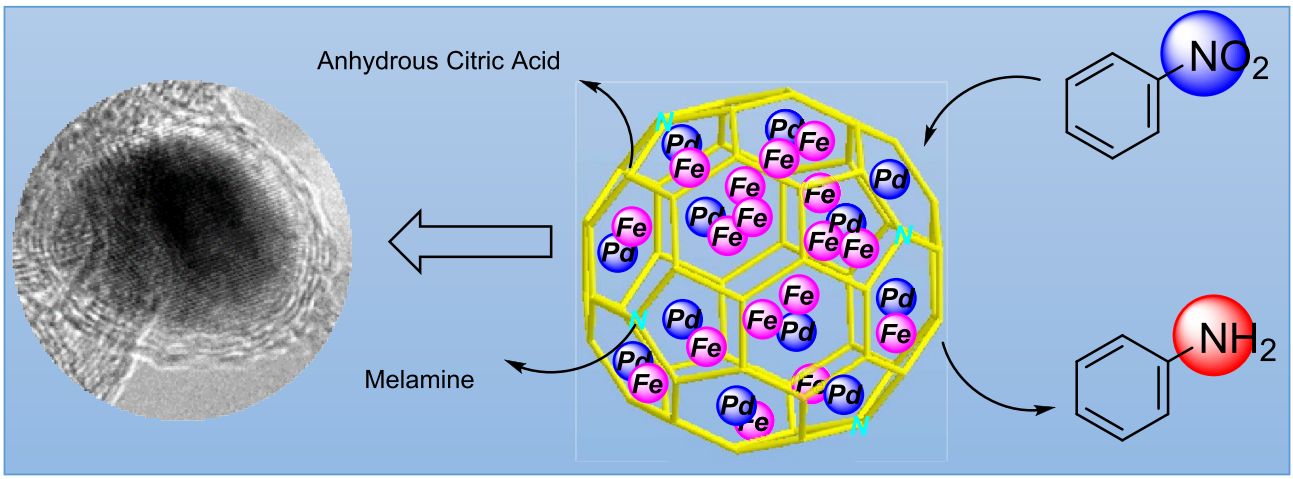

Keywords Nitrobenzene · Aniline · Hydrogenation · Heterogeneous catalyst · Transition metals · Graphene shelled catalyst

Shanshan Lin and Jianguo Liu have contributed equally to this work.

Extended author information available on the last page of the article

1 Introduction

Aniline, which serves as an important group of platform molecules, has been widely used in the synthesis of other high-value chemicals or products, such as polyurethane, dyes, rubber additives, explosives, medicines, pesticides, and fragrances [1, 2]. In particular, in the pharmaceutical field, aniline is widely used as an API. APIs, commonly known as raw materials for pharmaceuticals, are divided into two categories according to their sources: chemically synthesized drugs and natural chemical drugs. Chemical synthetic drugs can be divided into inorganic synthetic drugs and organic synthetic drugs. Inorganic synthetic drugs are inorganic compounds (very few are elements); organic synthetic drugs are mainly drugs made from basic organic chemical raw materials, through a series of organic chemical reactions (such as aspirin, chloramphenicol, caffeine, etc.). Natural chemical drugs can also be divided into two categories, according to their origin, biochemical drugs and phytochemical drugs. API, organic synthetic drugs, the largest proportion of varieties, production and output value, is the main pillar of the chemical pharmaceutical industry. The quality of raw materials to determine the quality of the preparation, so its quality standards are very strict requirements. Some amine drugs [3] for the prevention and treatment of diseases such as cardiovascular, cerebrovascular diseases, and cancer have always been occupied a high demand position in the market. For example, in the synthesis of Adempas (Riociguat), a drug used in the treatment of cardiovascular diseases (Fig. 1), aniline can be commonly used as a raw material for the starting reaction 2-Fluorobenzylhydrazine drug intermediate [4]. Most of the remaining synthetic methods also use aniline derivatives [5, 6] or directly as a raw material for the reaction route. Especially with the raging new coronavirus, how to produce high-value aniline drug intermediates more efficiently and environmentally in the industry has become a research hotspot [7].

Traditionally, nitrobenzene hydrogenation methods mainly include metals (Fe, Zn, Sn)/acid reduction method, sulfide reduction method, and catalytic hydrogenation method. However, the production process of the first two methods usually produces harmful substances, including metal salt slag and sulfur-containing wastewater [8–10], and such processes are affected by equipment corrosion and environmental pollution which are gradually replaced by more gentle procedures. Catalytic hydrogenation is an environmentally friendly method for preparing halogenated anilines. So far, the catalysts used for the hydrogenation of nitrobenzene are mainly noble Pt, Pd, Ru based catalysts, and some other non-noble Ni, Co and Fe based catalysts

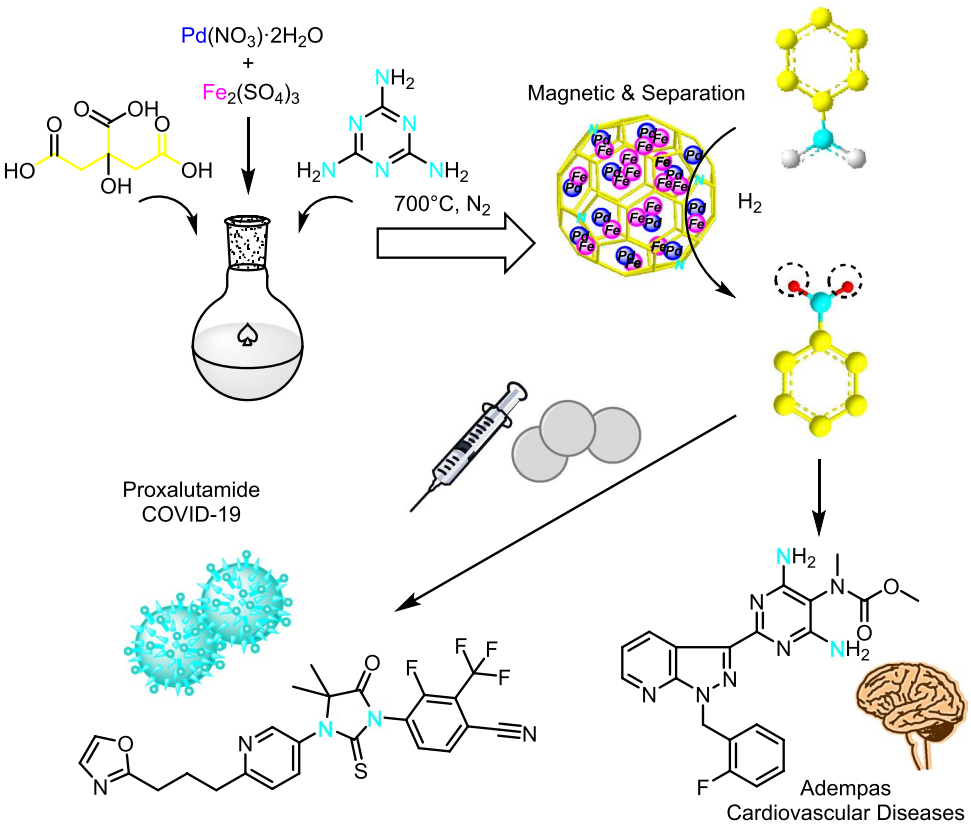

Fig. 1 Preparation of Pd/Fe@N/C catalyst and its application in the synthesis of drugs intermediate

[11–17]. In the case of hydrogen as the hydrogen donor, some precious metals are often used for direct hydrogenation of nitroaromatics under high temperature and high pressure [18, 19]. According to the catalyst formulation, some metal-based catalysts, especially Pd [20–22], showed good catalytic performance. However, the current trend in the pharmaceutical and food industries is the progress of economical, green, and environmentally friendly processes. It is very important and desirable to develop more cost-effective and practical application aniline synthesis methods. In order to improve the activity and recyclability of the catalyst, researchers immobilize nano-scale catalytically active metal Pd on various supports [23–25]. These heterogeneous catalysts showed good robustness and separability and had been used in industrial production, including fine chemical production. For the reduction of nitroaromatic compounds, doping of Pd has been reported to increase the catalytic activity of Fe_3O_4 substances [26]. In particular, the synergistic effect between Pd and Fe has been shown to be effective in the catalysis of nitro aromatic hydrocarbons to corresponding amines [27, 28].

As we all know, supported metal catalysts have attracted much attention because of their unique structure and better performance in certain catalytic reactions. Studies have shown that highly graphitized carbon promotes the reduction of nitrobenzene by enhancing electron transfer [29].

Strengthening the physical and chemical interaction between metal and metal-based catalyst support is one of the most effective methods to improve its catalytic performance in heterogeneous organic matter. Carbon materials have the advantages of flexibility for tailoring the pore structures and the potential for modification of the catalytic surface sites via introducing heteroatoms [30, 31]. Up to now, there have been several developed methods to modify the properties of carbon materials via activation with varied regents or doping with nitrogen, sulfur, phosphorus, etc. [32–36]. According to the report, N modification is expected to increase the activity and selectivity of the catalyst by introducing more anchor sites, adjusting the electronic structure of the central metal, and interacting with the active center of protons [37, 38]. The existence of N species in carbon materials changes the electronic state of carbon atoms and causes the graphite structure in carbon materials to expand and produce defect sites. These defect structures are essential for giving carbon materials superior catalytic activity and stability to selectively reduce nitrobenzene to aniline [39].

Herein, we prepared a Pd/Fe bimetallic catalyst supported on N-doped carbon materials to reduce nitrobenzene to aniline under mild reaction conditions. The Pd content is only 2.35wt% determined by ICP. Through the catalytic effect of Pd and Fe bimetals, the N-doped C support can provide more active sites, and the catalyst is easy to separate and recover. The Pd/Fe@N/C catalyst showed the best catalytic activity under mild reaction conditions of 0.8 MPa H_2 and 40 °C, achieving 99% nitrobenzene conversion and 99% aniline selectivity. Many halogen-substituted and aliphatic nitro compounds have been studied, and target products with excellent selectivity have been obtained. As the catalyst has magnetic properties and is easy to separate, the flow reactor process is considered for further exploration in the later stage. The excellent mass and heat transfer performance of the continuous flow process will further make the reaction conditions milder, and strive to achieve the conversion at room temperature.

2 Experimental Section

2.1 Materials

We bought the 1,3,5-trimethoxybenzene from Sigma Aldrich Co., Ltd., and $Pd(NO_3)_2{\cdot}2\ H_2O$ (AR, Pd 18.09 wt. % in nitric acid), $Fe_2(SO_4)_3$, $Fe_2(SO_4)_3$, anhydrous citric acid (AR, ≥ 99.5%), Melamine (AR, 99%), commercial single ruthenium atom nitrogen-doped carbon catalyst were obtained from Shanghai Macklin Biochemical Co., Ltd.; H_2SO_4 (GR, 98%) was purchased from Sinopharm Chemical Reagent Co., Ltd.; aniline (AR, ≥ 99.0%), methanol (AR, 99.7%), commercial single palladium atom nitrogen-doped carbon catalyst, Raney nickel catalyst (20 ~ 40 meshes) were purchased from Aladdin (Shanghai) Chemical Technology Co., Ltd.; nitrobenzene (AR, 98.0%) was purchased from Tokyo Chemical Industry Co., Ltd.; Deionized water ($\sigma < 5$ μS/m) was self-made in the laboratory.

2.2 Preparation of Pd/Fe@N/C Catalysts

Palladium (II) nitrate hexahydrate ($Pd(NO_3)_2{\cdot}2\ H_2O$), $Fe_2(SO_4)_3$ ($FeSO_4{\cdot}7H_2O$), melamine, and citric acid ($C_6H_8O_7$) were dissolved in anhydrous ethanol (50 mL) by different ratios. The mixture was then aged at 70 ℃ for 4 h under stirring (300 rpm) until to obtain a green bubble gel, followed by drying at 100 ℃ for 24 h in a drying oven to remove the excess solvent. The obtained green solid was then calcined at a fixed bed at 700 ℃ for 3 h under a high-purity N_2 (99.999%) flow of 40 mL·min^{-1}. The heating rate was controlled at 2 ℃·min^{-1}. The obtained black solids were treated in 1 M H_2SO_4 aqueous solution at 70 ℃ until the solution was colorless to remove the insecure and uncovered Pd particles. The black solids were then fully washed with deionized water until the pH of the waste solution was 7. Finally, the black solids were dried at − 48 ℃ for 12 h in a vacuum by using a freeze dryer. The dried black solids were marked as M1/M2 @ X/C, where M1 = Pd; M2 = Fe; X is the N doping, such as Pd/Fe@N/C.

2.3 Hydrogenation of Nitroarene in a Batch Reactor

The reaction was carried out in a batch reactor (Shanghai Yanzheng Instruments Co., Ltd.). In a typical run, the reaction solution (nitroarene (0.5 mmol) and (MeOH (6 mL)), catalyst (10 mg), and magnetic stirring bar were placed in a glass liner and then placed in the reactor. Then, the autoclave was sealed and purged with H_2 3 times under a pressure of 0.8 MPa, and pressurized with the set target H_2 pressure. The magnetic stirrer was rotated at a constant speed of 300 rpm throughout the whole period to ensure a homogeneous reaction. The autoclave was preheated from room temperature to the target reaction temperature (the internal temperature detected by the thermocouple) at a rate of 2 ℃·min^{-1}. The reaction was carried out at the reaction temperature for the required time. After the reaction, the autoclave was cooled to room temperature and the remaining gas was discharged. The reaction solution was collected with a dropper and filtered. The catalyst was fixed on a magnetic stir bar and washed thoroughly with methanol and water. Then used a freeze dryer to dry the catalyst (together with a magnetic stir bar) under vacuum at – 48 ℃ for 12 h. The reaction product was identified by GCMS, and the yield of the reaction product was determined and calculated by GCMS using 1,3,5-trimethoxybenzene as the internal standard.

3 Results and Discussion

3.1 Synthesis and Characterizations of Pd/Fe@N/C Catalysts

Figure 2 showed some representative scanning electron microscopy (SEM) images and transmission electron microscopy (TEM) images of nitrogen-doped graphene encapsulated Pd/Fe@N/C catalyst. As shown in Figs. 2a and b, the surface of the Pd/Fe@N/C catalyst had an obvious pore structure with the Pd and Fe particles dispersed evenly. The smaller Pd particles were evenly interspersed between the Fe particles, and the two particles were covered by a thin C shell to prevent the loss of the catalyst metal particles in the subsequent reaction. According to the HR-TEM analysis, the prepared N-doping Pd/Fe@N/C catalysts consisted of metal nanoparticles that were encapsulated by less than 5 graphene layers (Fig. 2c), and > 90% of metal species were encapsulated by a few graphene layers.

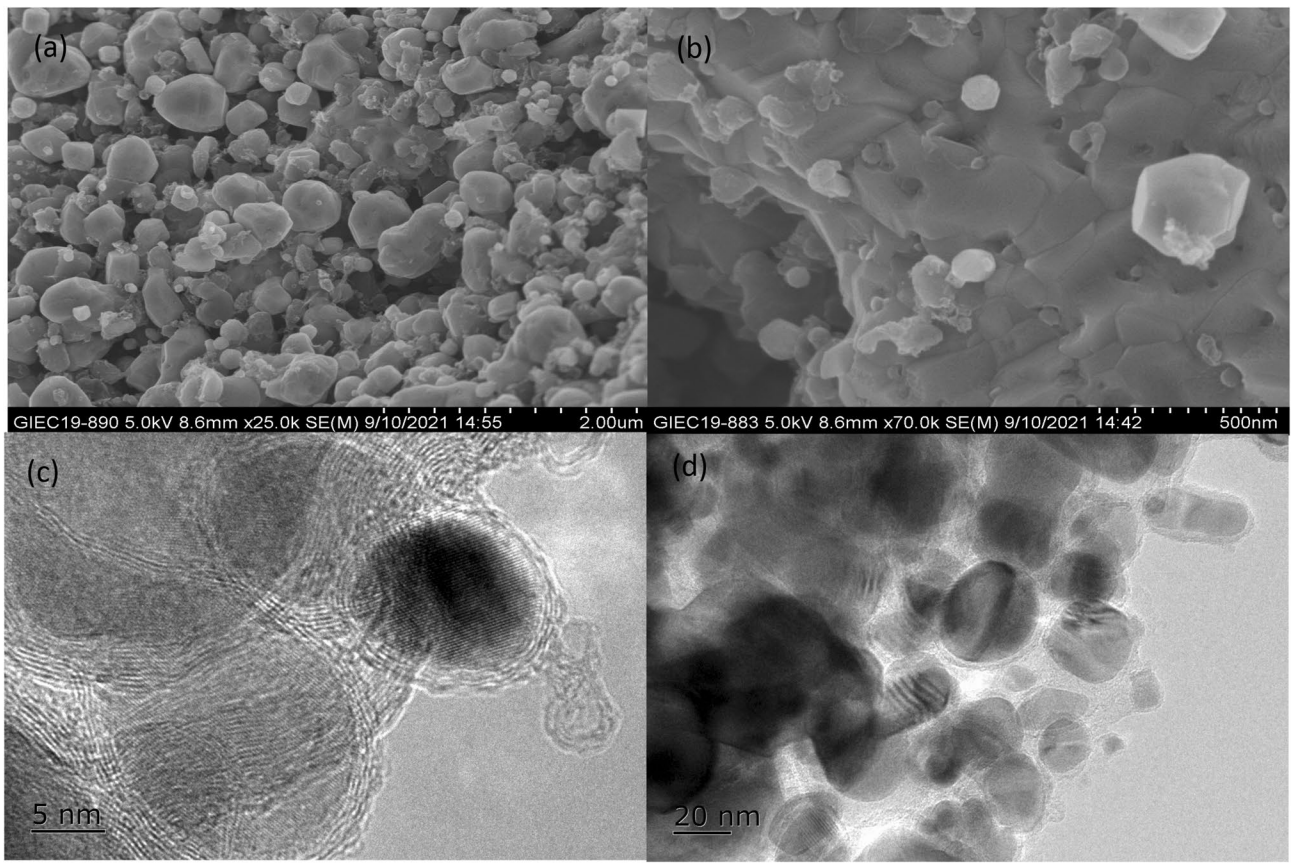

Fig. 2 Catalyst characterization. Representative SEM images and TEM images of Pd/Fe@N/C catalyst

In addition, X-ray photoelectron spectroscopy (XPS) was used to evaluate the detailed composition and elemental valence of Pd/Fe@N/C catalysts. The Pd/Fe@N/C catalyst is composed of carbon, nitrogen, oxygen, palladium and iron. As shown in Fig. 3a, the high-resolution c1s spectrum can show peaks with C–C/C = C bonds at 284.8 eV, respectively. Due to the incorporation of N, a peak of the C–N bond is shown at 286.3 eV. There are also 2 peaks around 288.6 and 290.8 eV, which can be attributed to C–O and O–C = O bonds, respectively. The N 1 s spectra were deconvolved into four peaks with binding energies of 394.6, 398.6, 400.8, and 404.2 eV, indicating that N atoms doped into C had four distinct bonding characteristics, in the form of pyridine-N, amine/M-Nx (demonstrating chemical coordination of N species and metals), pyrrole-N, and graphite-N (Fig. 3b). The 3d orbital peaks of Pd are located at 336.1 and 341.4 eV due to carbothermal reduction due to high-temperature treatment, which corresponds to 3d $_{5/2}$ and 3d $_{3/2}$ of metal Pd (0) (Fig. 3c). During the preparation and storage of the catalyst, Pd is oxidized to a certain extent, and it can also be seen from Fig. 3c that $3d_{5/2}$ and $3d_{3/2}$ of Pd (II) appear at the two low-intensity peaks of 338.1 and 344.5 eV. Similarly, it can be seen in Fig. 3d that Fe 2p behaves at two peaks at 711.7 and 722.8 eV, referring to Fe $2p_{3/2}$ and Fe $2p_{1/2}$.

The XRD spectrum showed that the graphitic carbon shell C (002) (ICDD: 00–041-1487) had a peak between 20 and 30, which confirmed that a thin graphene shell had been formed. Moreover, we could also observe the intensity peaks of Pd (011), Pd (020) (ICDD: 96-152-3107) and Fe_3O_4 species (ICDD: 03–065-3107), combined with the XPS results, which indicates the formation of Pd/Fe@N/C catalyst (Fig. 4). Among various modification strategies, the incorporation of different metals, especially the secondary active metals, into magnetic metal oxides has been shown to be effective in improving the catalytic performance [26].

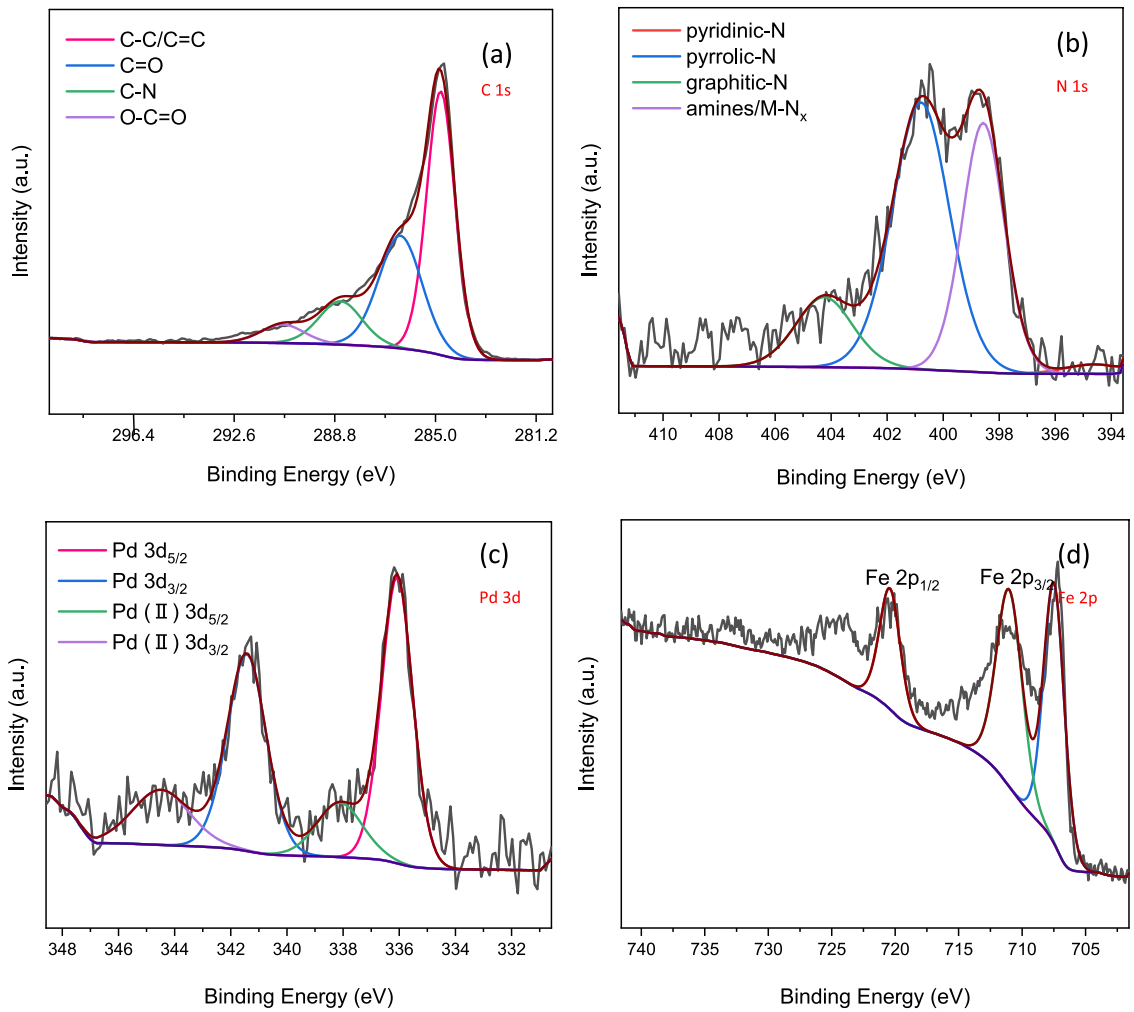

Fig. 3 XPS of Pd/Fe@N/C. **a** C 1 s spectrum of Pd/Fe@N/C; **b** N 1 s spectrum of Pd/Fe@N/C; **c** Pd 3d spectrum of Pd/Fe@N/C; and **d** Fe 2p spectrum of Pd/Fe@N/C

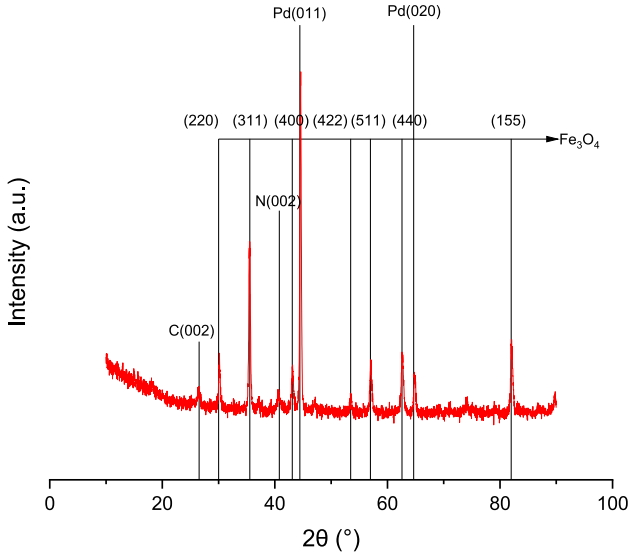

Fig. 4 XRD images of Pd/Fe@N/C catalyst

3.2 Pd/Fe@N/C Catalyzed Selective Hydrogenation of Nitroarenes

After the successful synthesis of the N-doped graphene encapsulated Pd and Fe bimetallic catalyst Pd/Fe@N/C, we then tested its catalytic reactivity for the reductive amination of nitrobenzene. Figure 5 showed the conversion rate and selectivity distribution of aniline at 1 MPa H_2 pressure and different temperatures. As shown in Fig. 5a, nitrobenzene produced many by-products during the reduction process at room temperature (25 °C), but only by raising the temperature to 40 °C the selectivity can be increased to 91.34% with a high catalytic activity. The increase in degree is accompanied by a conversion rate of 92.60%. Similarly, during pressure screening, we found that many by-products are still generated at a hydrogen pressure of 0.1 bar. As shown in Fig. 5b, the overall conversion and selectivity are optimal at a hydrogen pressure of 0.8 bar. It is worth noting that the conversion rate of nitrobenzene at a pressure of 0.8 MPa is higher than that at a pressure of 1 MPa. This is because competitive adsorption partly weakens the bond between each adsorbate and the surface. Specifically, it is due to the competitive adsorption of phenyl and N-containing groups in the process of $PhNO_2$ hydrogenation. The weak bond between the adsorbate and the surface is more conducive to association reactions such as hydrogenation. Since hydrogenation usually requires energy to partially destroy the bond between intermediate and surface atoms to form the bond between intermediate and hydrogen, the weaker the bond between intermediate and surface atoms, the lower the hydrogenation barrier. Therefore, the hydrogenation barrier becomes lower under actual reaction conditions.

Interestingly, the solvent has a great influence on the reduction of nitrobenzene. In the solvent range of Table1 Entry 1 ~ 7, only when the solvent is alcohols (Entry 1, 2, and 3) can the catalyst have a reduction effect on nitrobenzene. To explore whether hydrogen and methanol are used as a common source of hydrogen, we conducted a set of control experiments (Entry 8). The reductive amination of nitrobenzene was carried out with methanol as a solvent under a nitrogen pressure of 0.8 bar. It was found that no product aniline was formed, which shows that H_2 is true as the only hydrogen source. The solvent can not only promote the dispersion of the reactants and enhance the mass transfer process in the catalytic reaction but also change the path of the reaction kinetics [40]. Differences in the solubility of adsorbed hydrogen can cause significant differences in reactivity. In addition, the polarity of solvent can effectively

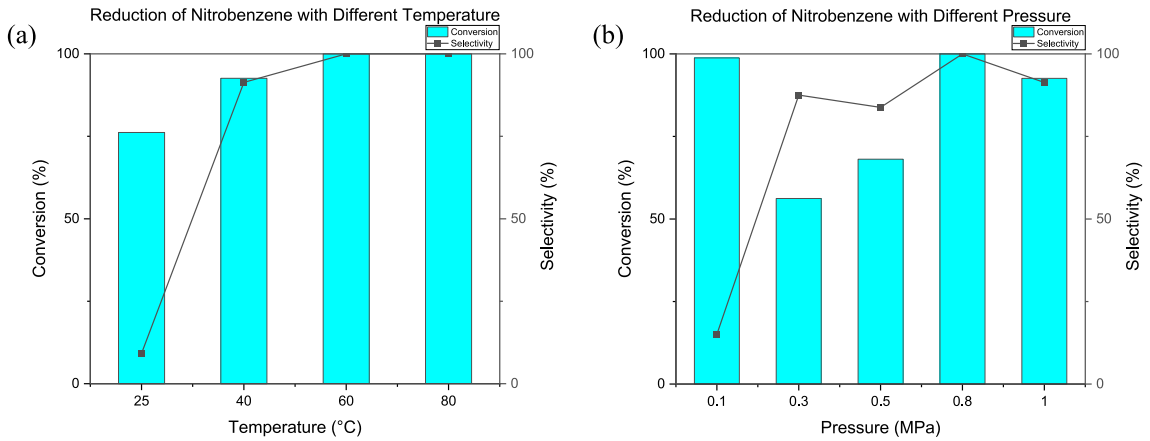

Fig. 5 Research on the reaction factors of Pd/Fe@N/C catalyzed hydrogenation of nitrobenzene. Reaction conditions: **a** Reaction conditions: 10 mg catalyst Pd/Fe@N/C, 0.05 mmol/L nitrobenzene (solvent: methanol), 1 MPa H_2, different reaction temperatures; **b** Reaction conditions: 10 mg catalyst Pd/Fe@N/C, 0.05 mmol/L nitrobenzene (solvent: methanol), different H_2 pressure, 40 °C; conversion rate and selectivity are determined by GC, using 1, 3, 5-trimethoxy Benzene is used as an internal standard

Table 1 Pd/Fe@N/C catalyzed nitrobenzene hydrogenation catalyst, solvent, and pressure type influence research

Entry	Cat	Solv	Temp. (°C)	Pre. (MPa)	Time (h)	Conv. (%)	Sel. (%)
1	Pd/Fe@N/C	**MeOH**	40	0.8	4	> 99	> 99
2	Pd/Fe@N/C	**EtOH**	40	0.8	4	12.72	78.95
3	Pd/Fe@N/C	**IPA**	40	0.8	4	6.03	90.65
4	Pd/Fe@N/C	DCM	40	0.8	4	–	–
5	Pd/Fe@N/C	TOL	40	0.8	4	–	–
6	Pd/Fe@N/C	EtOAc	40	0.8	4	–	–
7	Pd/Fe@N/C	CYH	40	0.8	4	–	–
8	Pd/Fe@N/C	MeOH	40	0.8[a]	4	–	–

[a]The source of pressure is N_2 instead of H_2

Bold indicates that the solvent is classified as an alcohol solvent

adjust the bonding between reactant/intermediate and Pd [41]. The hydrogenation kinetics of nitro compounds on palladium catalyst supported on coal was studied [42–44]. Klyuev [42] found that the hydrogenation of nitrobenzene is a first-order reaction for catalyst and hydrogen, and a pseudo-zero-order reaction for nitrobenzene. So the significant influence of the solvent is assumed to be due to the sol pores changing the adsorption configuration of reducing groups on the transition metal surface [45], changed the potential energy field formed by the hydrogen bond between the original solvent and the organic matrix [46–48]. It can be concluded that the hydrogen bond with the metal is weaker to a certain extent, which is beneficial to the hydrogenation rate, and it is consistent with the phenomenon in the pressure screening process.

In addition to the screening of reaction conditions, we also prepared some catalysts for control reactions showed in Fig. 6a. The results showed that although the amount of active metal Pd was reduced to 10% equivalent of Pd@N/C catalyst, the catalytic hydrogenation activity of p-nitrobenzene was greatly improved due to the bimetallic catalytic effect of transition metal Fe. However, when pure Fe was used as the active center, no matter what the valence state of the Fe central atom is, the catalytic hydrogenation of p-nitrobenzene cannot be exerted. In addition, by performing N doping on Fe@C catalysts for reaction comparison, we found that N doping did not play a role in the absence of Pd atoms, while in the bimetallic system, by doping Pd/Fe@C with N atoms, it was found that the catalytic activity of the doped catalyst was significantly improved. It is worth mentioning that after N doping the C support, the proportion of Pd/Fe bimetallic active components is relatively lower, even so, its catalytic activity still achieves the best. Therefore, both Pd and Fe metals play an indispensable role and greatly improve the catalytic activity while reducing the content of the noble metal Pd to a great extent. Therefore,

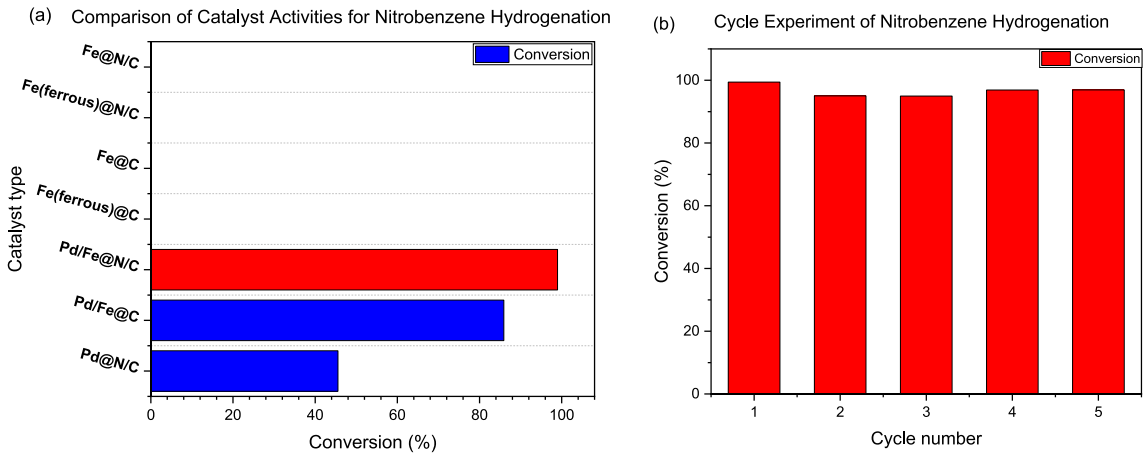

Fig. 6 Catalyst activity comparison and cycle performance research for nitrobenzene hydrogenation. **a**. The prepared series of catalysts comparison for the catalytic activity of nitrobenzene hydrogenation. The total amount of metal Pd and Fe added as the active center of the catalyst remained the same, in which the addition amount of Fe is ten times that of Pd. The Fe source of Fe (ferrous)@C series catalysts is $FeSO_4{\cdot}7H_2O$, and the Fe sources of the other catalysts are $Fe_2(SO_4)_3$. **b**. Pd/Fe@N/C catalyst catalyzed hydrogenation cycle experiment of nitrobenzene

the high catalytic efficiency of palladium-iron catalysts for nitrobenzene compounds can be attributed to the synergistic effect of palladium and iron [49]. Further DFT calculations were carried out by Wang's team to investigate the synergistic effect of Pd-Fe coupling on the electronic structure of each n-doped graphene model [50]. DFT results showed that the combination of Pd and Fe resulted in a significant decrease in energy, and the combined structure was more stable than that of single metal catalysts. The modified Pd-Fe nanoparticles can directly change the electronic structure of NC, and the introduction of metal nanoparticles can significantly improve the electrical conductivity of carbon and nitrogen around NC which is consistent with the experimental results shown in Pd/Fe@C in Fig. 6a. Because the spin density plays a leading role in improving the catalytic performance, DFT results show that the spin density volume of NC/PdFe is much larger than that of corresponding single metal catalysts. This phenomenon directly indicates that the formation of Pd-Fe alloy plays a key synergistic role in the enhancement of catalyst activity.

We carried out the cycle test on the prepared Pd/Fe@N/C catalyst as shown in Fig. 6b, and the results showed that the conversion rate of the catalyst for the hydrogenation of nitrobenzene was still greater than 95% after five cycle experiments. We performed ICP testing on the recycled catalyst and found that the Pd element content was 2.21%, and compared with the Pd content of 2.35% in the original catalyst, no significant metal loss occurred. It shows that under the loading of C shell, the catalytically active metal is well protected, which makes the catalyst have stable catalytic activity, resulting in a significant increase in the utilization rate of metal active centers. The reduction of nitro-aromatic compounds has been successfully applied in fixed-bed systems due to the low metal loss and easy magnetic separation of the catalysts [51]. For more efficient application in industrial systems, our work will be developed toward the flow system.

We have also studied many halogen-substituted and aliphatic nitro compounds and obtained target products with excellent selectivity (Fig. 7). Both industrially relevant and structurally challenging nitrobenzene derivatives have achieved effective amination, and the corresponding aniline has been produced in good to excellent yields. Fluoride and chloride substrates are well tolerated, but bromide substrates undergo more severe dehalogenation. Aliphatic nitro compounds can also withstand the reaction conditions, and the corresponding anilines can be obtained with excellent yields. Even cycloalkyl nitro compounds with various ring sizes can be successfully transferred to aniline.

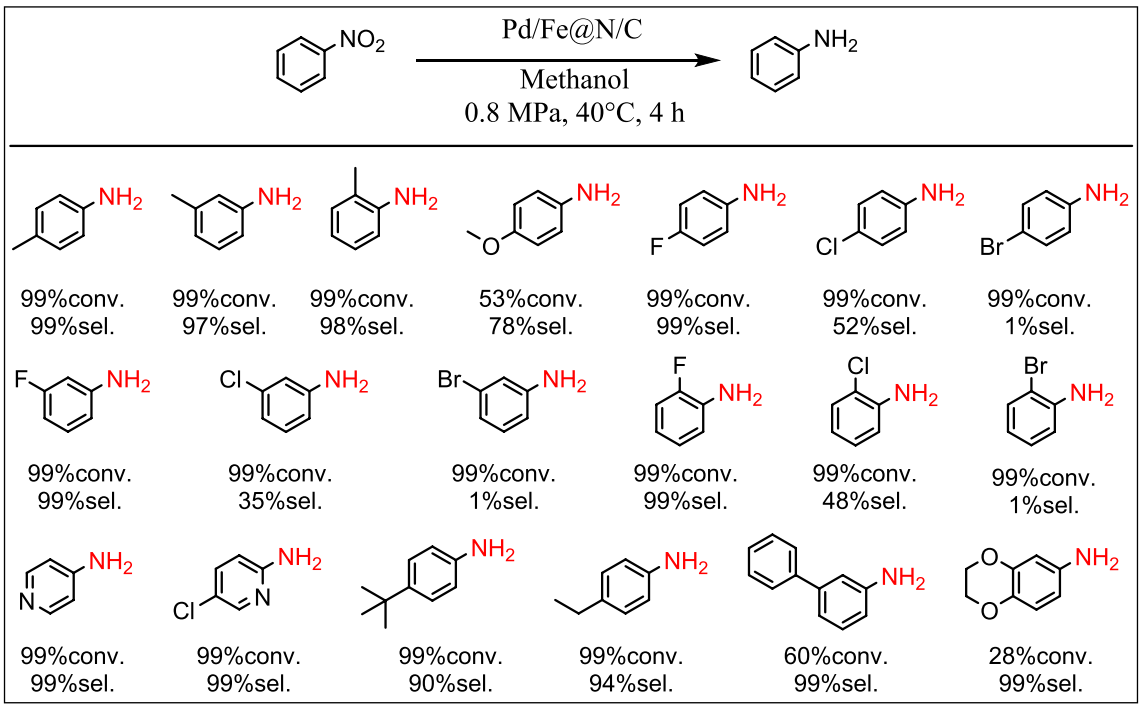

Fig. 7 Reaction conditions: 10 mg catalyst Pd/Fe@N/C, 0.05 mmol/L nitrobenzene (solvent: methanol), 0.8 MPa H_2, 40 °C; conversion rate and selectivity are determined by GC–MS, using 1, 3, 5-trimethoxy benzene is used as an internal standard

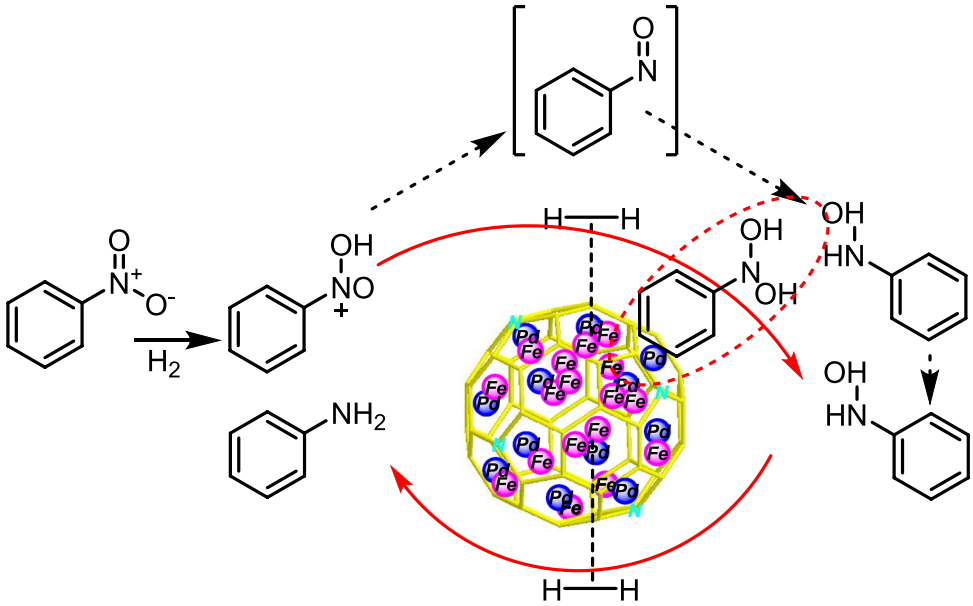

Fig. 8 Proposed mechanism of Pd/Fe@N/C catalytic hydrogenation of nitrobenzene to aniline. The dashed path indicates the Hubble direct path, and the red path indicates the broken key path

3.3 Proposed Mechanism of Pd/Fe@N/C Catalyzed Hydrogenation of Nitrobenzene

Based on the above experiments and analysis, a proposed mechanism was proposed as illustrated in Fig. 8. Unlike the previously reported Haber reaction mechanism [52], the reduction of nitrobenzene could be achieved through the phenylhydroxylamine (PhNHOH) intermediate but not via the PhNO intermediate [53–55]. First, the substrate was absorbed on the catalyst active species and the N–O bond was activated and broke with the help of Pd-H species. Then the formed PhNOOH* intermediate could directly undergo hydroxyl elimination reaction to produce the PhNO* intermediate, or it could be further reduced to form $PhN(OH)_2$* intermediate, which was further subjected to dehydroxylated reaction to form the PhNOH* intermediate. It has been known that the highest energy barrier required for the hydrogenation of PhNHOH* intermediate to PhNH* intermediate is the rate determining step for the final reduction of hydroxylamine intermediate to aniline. However, based on the above experimental studies, we found that if the hydrogen pressure was too high, the activated H* might occupy the reactive sites of the catalyst, thereby hindering the dissociation reaction of the N–O bond to a certain extent, and forming intermediates that were more difficult to dissociate.

We also verified the above hypothesized mechanism by examining the compositional changes during the reaction at different times (Fig. 9). In the early stage of the reaction, the catalyst did not convert nitrobenzene to aniline in one step, but first generated azobenzene and azobenzene oxide which were the condensation product of the intermediate, and then gradually hydrogenated to aniline. This also confirms the above proposed mechanistic route. After almost complete conversion of nitrobenzene to the intermediate, the intermediate components are rapidly hydrogenated, while the rate of aniline formation is greatly accelerated.

4 Conclusion

We prepared a Pd/Fe magnetic bimetallic catalyst supported on N-doped carbon materials to reduce nitrobenzene to aniline under mild conditions without the formation of by-products. The Pd content is only 2.35wt%. Through the catalytic effect of Pd and Fe bimetals, the N-doped graphene support can provide more active sites, and the magnetic catalyst is easy to separate and easy to recover. For the hydrogenation of nitro compounds, Pd/Fe@N/C shows the best catalytic activity under mild reaction conditions of 0.8 MPa H_2 and 40 °C, achieving 99% nitrobenzene conversion and 99% aniline selection. Many halogen-substituted and aliphatic nitro compounds have been studied, and target products with excellent selectivity have been obtained. Because the catalyst is magnetic and easy to separate, the flow reactor system is considered for further exploration in the later stage. The excellent mass and heat transfer performance of the flow reactor system will further make the reaction conditions milder, and strive to achieve the conversion at room temperature.

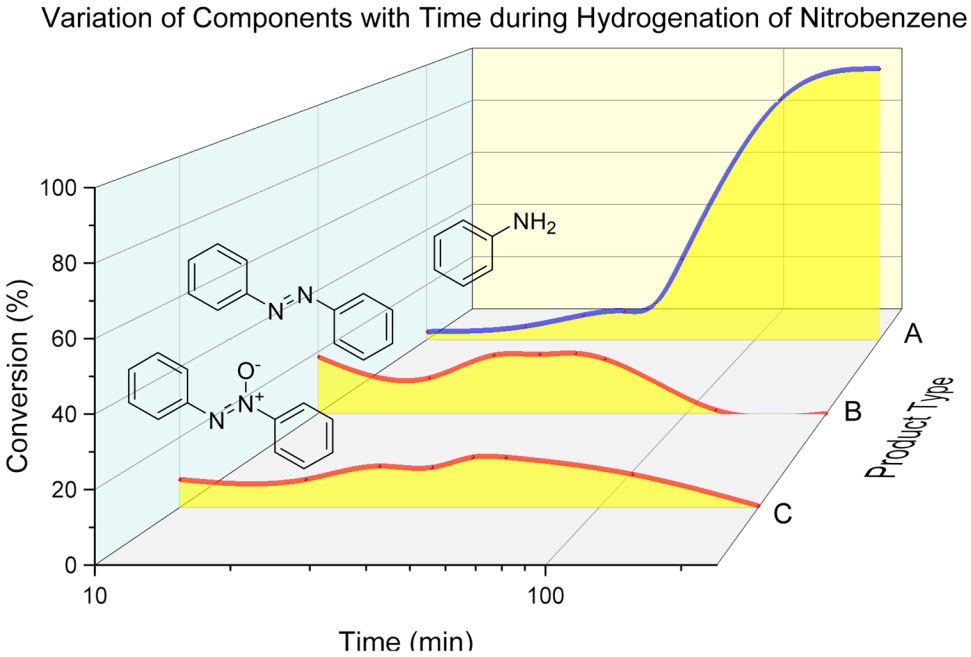

Fig. 9 Detection of intermediate components during the reaction of Pd/Fe@N/C catalytic hydrogenation of nitrobenzene to aniline

Supplementary Information The online version contains supplementary material available at https://doi.org/10.1007/s10562-023-04273-7.

Acknowledgements This work was supported financially by National Natural Science Foundation of China (52236010, 51976225) and Fundamental Research Funds for the Central Universities (2242022R10058).

Author contributions J. G. L. supervised and designed the research. S.S.L. performed the experiments and data analysis. S.S.L. and J. G. L. co-wrote the original manuscript. J.G.L. reviewed and corrected the manuscript. All authors discussed the results and assisted during manuscript preparation.

Data availability Data supporting the findings of this study are available from the corresponding authors upon reasonable request.

Declarations

Competing interests The authors declare no competing financial interests.

References

1. Johannsen M, Jorgensen KA (1998) Allylic amination. Chem Rev 98(4):1689–1708
2. Natte K, Jagadeesh RV, Sharif M, Neumann H, Beller M (2016) Synthesis of nitriles from amines using nanoscale Co3O4-based catalysts via sustainable aerobic oxidation. Org Biomol Chem 14(13):3356–3359
3. J. Njarðarson, Top 200 Small Molecule Pharmaceuticals by Retail Sales in 2018.
4. An expeditious synthesis of riociguat (2013) A pulmonary hypertension drug. Der Pharma Chemica 5:232–239
5. Wang H, Deng Q, Yuan B (2016) Synthesis of riociguat. Chinese J Pharm 47(6):675–678
6. Liang LI, Xingzhou LI, Yadan LIU, Zhibing Z, Song LI (2011) Synthesis of riociguat in the treatment of pulmonary hypertension. Chinese J Med Chem 21(2):120–125
7. Flávio C, Fonseca D, Mccoy J, Zimerman RA, Goren A (2021) Efficacy of proxalutamide in hospitalized COVID-19 patients: a randomized double-blind placebo-controlled, parallel-design clinical. Trial MedRxiv. https://doi.org/10.1101/2021.06.22.21259318
8. Burawoy A, Critchley JP (1959) Electronic spectra of organic molecules and their interpretation .5. Effect of terminal groups containing multiple bonds on the k-bands of conjugated systems. Tetrahedron 5(4):340–351
9. Sidgwick NV, Rubie HE (1921) The solubility and volatility of the chloro- and nitro-anilines and of their acetyl derivatives. J Chem Soc 119:1013–1024
10. Scientific and Industrial Notes (1926) J Soc Dye Colour 42(8):254–254
11. Zhu W, Chen L, Hu CD, Hu LQ (2005) Analysis on pressure distribution in HT-7 neutral beam injection system. Plasma Sci Technol 7(2):2719–2722
12. Zuo BJ, Wang Y, Wang QL, Zhang JL, Wu NZ, Peng LD, Gui LL, Wang XD, Wang RM, Yu DP (2004) An efficient ruthenium catalyst for selective hydrogenation of ortho-chloronitrobenzene prepared via assembling ruthenium and tin oxide nanoparticles. J Catal 222(2):493–498
13. Liang JF, Zhang XM, Jing LY, Yang HQ (2017) N-doped ordered mesoporous carbon as a multifunctional support of ultrafine Pt nanoparticles for hydrogenation of nitroarenes. Chinese J Catal 38(7):1252–1260
14. Meng XC, Cheng HY, Akiyama Y, Hao YF, Qiao WB, Yu YC, Zhao FY, Fujita S, Arai M (2009) Selective hydrogenation of nitrobenzene to aniline in dense phase carbon dioxide over Ni/gamma-Al2O3: Significance of molecular interactions. J Catal 264(1):1–10
15. Zhuang QQ, Cao JP, Wu Y, Zhao M, Zhao XY, Zhao YP, Bai HC (2021) Heteroatom nitrogen and oxygen co-doped

three-dimensional honeycomb porous carbons for methylene blue efficient removal. Appl Surf Sci 546:149139
16. Tian M, Cui XL, Yuan M, Yang J, Ma JT, Dong ZP (2017) Efficient chemoselective hydrogenation of halogenated nitrobenzenes over an easily prepared gamma-Fe2O3-modified mesoporous carbon catalyst. Green Chem 19(6):1548–1554
17. Wei Q, Shi YS, Sun KQ, Xu BQ (2016) Pd-on-Si catalysts prepared via galvanic displacement for the selective hydrogenation of para-chloronitrobenzene. Chem Commun 52(14):3026–3029
18. Feng YG, Xu WW, Huang BL, Shao Q, Xu L, Yang SZ, Huang XQ (2020) On-demand, ultraselective hydrogenation system enabled by precisely modulated pd-cd nanocubes. J Am Chem Soc 142(2):962–972
19. Ye TN, Xiao Z, Li J, Gong YT, Abe H, Niwa Y, Sasase M, Kitano M, Hosono H (2020) Stable single platinum atoms trapped in sub-nanometer cavities in 12CaO center dot 7Al(2)O(3) for chemoselective hydrogenation of nitroarenes. Nat Commun 11(1):1–10
20. Chen G, Zhu X, Chen R, Liao Q, Ye DD, Feng H, Liu J, Liu M (2018) Gas-liquid-solid monolithic microreactor with Pd nanocatalyst coated on polydopamine modified nickel foam for nitrobenzene hydrogenation. Chem Eng J 334:1897–1904
21. Hajiahmadi Z, Tavangar Z (2018) Investigating the adsorption of nitrobenzene on M/Pd (111) bimetallic surface as an effective catalyst. Appl Surf Sci 454:343–349
22. Tokai A, Okitsu K, Hori F, Mizukoshi Y, Nishimura Y, Seino S, Iwase A (2017) One-pot preparation of Pd nanoparticles supported on graphene from Pd electrodes by discharge plasma in graphene suspension and its catalytic activity for hydrogenation of nitrobenzene. Mater Lett 199:24–27
23. Jiang WD, Xu B, Xiang Z, Liu XQ, Liu F (2016) Preparation and reactivity of UV light-reduced Pd/alpha-Fe2O3 catalyst towards the hydrogenation of o-chloronitrobenzene. Appl Catal a-Gen 520:65–72
24. Shi YS, Yuan ZF, Wei Q, Sun KQ, Xu BQ (2016) Pt-FeOx/SiO2 catalysts prepared by galvanic displacement show high selectivity for cinnamyl alcohol production in the chemoselective hydrogenation of cinnamaldehyde. Catal Sci Technol 6(19):7033–7037
25. Liu HM, Tao K, Xiong CR, Zhou SH (2015) Controlled synthesis of Pd-NiO@SiO2 mesoporous core-shell nanoparticles and their enhanced catalytic performance for p-chloronitrobenzene hydrogenation with H-2. Catal Sci Technol 5(1):405–414
26. Wen LS, Wang D, Xi JB, Tian F, Liu P, Bai ZW (2022) Heterometal modified Fe3O4 hollow nanospheres as efficient catalysts for organic transformations. J Catal 413:779–785
27. Zhang Y, Huang J, Dong ZX, Zhan Y, Xi JB, Xiao J, Huang SH, Tian F (2022) Pd-Fe bimetallic nanoparticles anchored on N-doped carbon-modified graphene for efficient catalytic organic reactions. Carbon Lett. https://doi.org/10.1007/s42823-022-00404-z
28. Wang D, Jiangbo J, Zhengwu J (2019) Pd-Fe dual-metal nanoparticles confined in the interface of carbon nanotubes/N-doped carbon for excellent catalytic performance. Appl Surf Sci 489(1):477–484
29. Wei CH, Yin SJ, Zhu DQ (2020) Mechanisms for sulfide-induced nitrobenzene reduction mediated by a variety of different carbonaceous materials: graphitized carbon-facilitated electron transfer versus quinone-facilitated formation of reactive sulfur species. J Environ Qual 49(6):1564–1574
30. Laine J, Labady M, Severino F, Yunes S (1997) Sink effect in activated carbon-supported hydrodesulfurization catalysts. J Catal 166(2):384–387
31. Wu Y, Cao JP, Zhuang QQ, Zhao XY, Zhou Z, Wei YL, Zhao M, Bai HC (2021) Biomass-derived three-dimensional hierarchical porous carbon network for symmetric supercapacitors with ultrahigh energy density in ionic liquid electrolyte. Electrochim Acta 371:137825
32. Deng DH, Novoselov KS, Fu Q, Zheng NF, Tian ZQ, Bao XH (2016) Catalysis with two-dimensional materials and their heterostructures. Nat Nanotechnol 11(3):218–230
33. Gupta N, Khavryuchenko O, Villa A, Su DS (2017) Metal-free oxidation of glycerol over nitrogen-containing carbon nanotubes. Chemsuschem 10(15):3030–3034
34. Wu Y, Cao JP, Zhou Z, Zhao XY, Zhuang QQ, Wei YL, Zhao M, Zhao YP, Bai HC (2020) Transforming waste sugar solution into N-doped hierarchical porous carbon for high performance supercapacitors in aqueous electrolytes and ionic liquid. Int J Hydrogen Energ 45(56):31367–31379
35. Inagaki M, Toyoda M, Soneda Y, Morishita T (2018) Nitrogen-doped carbon materials. Carbon 132:104–140
36. Ma RG, Zhou Y, Chen YF, Li PX, Liu Q, Wang JC (2015) Ultrafine molybdenum carbide nanoparticles composited with carbon as a highly active hydrogen-evolution electrocatalyst. Angew Chem Int Edit 54(49):14723–14727
37. To JWF, He JJ, Mei JG, Haghpanah R, Chen Z, Kurosawa T, Chen SC, Bae WG, Pan LJ, Tok JBH, Wilcox J, Bao ZN (2016) Hierarchical N-doped carbon as CO2 adsorbent with high CO2 selectivity from rationally designed polypyrrole precursor. J Am Chem Soc 138(3):1001–1009
38. Zh A, Jin LA, Qw B, Meng ZA, Zw A, Jc A, Dm B, Cx B, Jx A, Jy A (2019) Metal-free carbocatalyst for catalytic hydrogenation of N-containing unsaturated compounds. J Catal 377:199–208
39. Xu Q, Gao GM, Tian HL, Gao ZR, Zhang S, Xu LL, Hu X (2021) Carbon materials derived from polymerization of bio-oil as a catalyst for the reduction of nitrobenzene. Sustain Energ Fuels 5(11):2952–2959
40. Cheng G, Jentys A, Gutiérrez OY, Liu Y, Chin Y-H, Lercher JA (2021) Critical role of solvent-modulated hydrogen-binding strength in the catalytic hydrogenation of benzaldehyde on palladium. Nat Catal 4(11):976–985
41. Chen XD, Shen K, Ding DN, Chen JY, Fan T, Wu RF, Li YW (2018) Solvent-driven selectivity control to either anilines or dicyclohexylamines in hydrogenation of nitroarenes over a bifunctional Pd/MIL-101 catalyst. Acs Catal 8(11):10641–10648
42. Klyuev MV (1987) Influence of substituents in nucleus on hydration of aromatic nitrocompounds in the presence of metal-complex catalysts. Zh Org Khim+ 23(3):581–585
43. Belyaev SV, Nasibulin AA, Klyuev MV (1999) The effect of character of double bonds in organic compounds on their rate of hydrogenation over a palladium-containing ion-exchanger. Petrol Chem 39(4):267–270
44. Nakao Y, Fujishige S (1981) Colloidal nickel boride catalyst for hydrogenation of olefins. J Catal 68(2):406–410
45. Xia H, Tan HZ, Cui HY, Song F, Zhang Y, Zhao RR, Chen ZN, Yi WM, Li ZH (2021) Tunable selectivity of phenol hydrogenation to cyclohexane or cyclohexanol by a solvent-driven effect over a bifunctional Pd/NaY catalyst. Catal Sci Technol 11(5):1881–1887
46. Herrerias CI, Yao XQ, Li ZP, Li CJ (2007) Reactions of C-H bonds in water. Chem Rev 107(6):2546–2562
47. Butler RN, Coyne AG (2010) Water: nature's reaction enforcer-comparative effects for organic synthesis "in-water" and "on-water." Chem Rev 110(10):6302–6337
48. Akpa BS, D'Agostino C, Gladden LF, Hindle K, Manyar H, McGregor J, Li R, Neurock M, Sinha N, Stitt EH, Weber D, Zeitler JA, Rooney DW (2012) Solvent effects in the hydrogenation of 2-butanone. J Catal 289:30–41
49. Zhang N, Qiu Y, Sun HY, Hao JF, Chen J, Xi JB, Liu J, He BJ, Bai ZW (2021) Substrate-assisted encapsulation of pd-fe bimetal nanoparticles on functionalized silica nanotubes for catalytic hydrogenation of nitroarenes and azo dyes. Acs Appl Nano Mater 4(6):5854–5863
50. Xi JB, Wang QJ, Duan XM, Zhang N, Yu JX, Sun HY, Wang S (2021) Continuous flow reduction of organic dyes over Pd-Fe

alloy based fibrous catalyst in a fixed-bed system. Chem Eng Sci 231:116303
51. Hu H, Du S, Xi J (2022) N-Doped holey graphene assembled on fibrous aluminum silicate for efficient carbocatalysis in fixed-bed systems. Green Chem 24(13):5255–5262
52. Haber F (1898) Gradual electrolytic reduction of nitrobenzene with limited cathode potential. Elektrochem Angew Phys Chem 22:506–514
53. Corma A, Concepcion P, Serna P (2007) A different reaction pathway for the reduction of aromatic nitro compounds on gold catalysts. Angew Chem Int Edit 46(38):7266–7269
54. Gelder EA, Jackson SD, Lok CM (2005) The hydrogenation of nitrobenzene to aniline: a new mechanism. Chem Commun 4:522–524
55. Visentin F, Puxty G, Kut OM, Hungerbuhler K (2006) Study of the hydrogenation of selected nitro compounds by simultaneous measurements of calorimetric, FT-IR, and gas-uptake signals. Ind Eng Chem Res 45(13):4544–4553

Authors and Affiliations

Shanshan Lin[1,3] · Jianguo Liu[2] · Longlong Ma[2]

✉ Jianguo Liu
liujg@seu.edu.cn

[1] CAS Key Laboratory of Renewable Energy, Guangdong Provincial Key Laboratory of New and Renewable Energy Research and Development, Guangzhou Institute of Energy Conversion, Chinese Academy of Sciences, Guangzhou 510640, People's Republic of China

[2] Key Laboratory of Energy Thermal Conversion and Control of Ministry of Education, School of Energy and Environment, Southeast University, Nanjing 210096, People's Republic of China

[3] University of Chinese Academy of Sciences, Beijing 100049, People's Republic of China